IEEE Access
Multidisciplinary | Rapid Review | Open Access Journal

Received May 4, 2019, accepted May 24, 2019, date of publication June 10, 2019, date of current version August 20, 2019.

Digital Object Identifier 10.1109/ACCESS.2019.2922150

On Biologically Inspired Stochastic Reinforcement Deep Learning: A Case Study on Visual Surveillance

NADINE HAJJ AND MARIETTE AWAD
Department of Electrical and Computer Engineering, American University of Beirut, Beirut 11-0236, Lebanon

Corresponding author: Mariette Awad (mariette.awad@aub.edu.lb)

This work was supported by the American University of Beirut Research Board and the Angela and Munib Masri Institute at the American University of Beirut.

ABSTRACT Here, we present a biologically inspired visual network (BIVnet) for image processing tasks. The proposed model possesses similarities with its neural counterpart and is trained by a stochastic algorithm which employs a partially observable Markov decision process to execute a reinforcement learning strategy. The network was tested on a collection of available datasets in surveillance-related tasks and showed superior performance compared with the state-of-the-art architectures. An average improvement of 15.2% in accuracy on a collection of publicly available image datasets is shown in our experimental results.

INDEX TERMS Abandoned luggage detection, deep learning, person identification, visual tasks.

I. INTRODUCTION

In an era where an average internet user generates around 1.5 gigabytes of data per day, methods for effective data mining, such as those involving machine learning, become critical. With the tremendous increase in computational power provided by the development of GPUs and other distributed architectures, deep learning has attained considerable success in a variety of computer vision tasks, including but not limited to facial recognition, object identification and scene understanding. One field that has benefited tremendously from the evolution of deep learning algorithms is security applications. With convolutional neural networks exceeding human performance levels [1] in the ImageNet LSVRC 2010 context, various sets of convolutional architectures are now ready-made for use in image-related machine learning tasks. Such models have been widely and successfully employed for tasks such as facial detection [2], [3], person re-identification [4]–[6], abandoned luggage detection in airports and public settings [7], [8], and criminal event classification [9]–[11].

While cameras are widely installed in areas ranging from commercial shops to airports and streets, the sense of security among the general populace remains low due to increasing threats from malicious individuals or groups and the lack of constant monitoring of these cameras. While ensuring around the clock surveillance staff may be expensive and impractical, implementing intelligent systems that utilize deep learning and are capable of detecting security breaches and/or recognizing suspects is an efficient and desirable solution.

While computationally demanding, the burden of training such models is alleviated by the use of distributed platforms - a phase which generally occurs offline - and performing the testing phase online provided sufficient resources are available for storage and processing. However, despite the considerable performance that pre-trained models can achieve, a fine tuning stage is often required to adapt the model to the particularity of the dataset. Another challenge is posed by the generally low resolution of surveillance images, in addition to the fast response time generally required when responding to security threats. In the face of these vexing tasks, more solutions are needed to meet the taxing requirements of today's security threats.

In this paper, we present BIVnet (Biologically Inspired Visual network), a visual processing deep network inspired by the human visual system which encompasses the eye, the lateral geniculate nucleus and the primary visual cortex. We also present a stochastic reinforcement learning algorithm based on spike-timing-dependent plasticity. Our network was tested on three security-related tasks: person re-identification,

The associate editor coordinating the review of this manuscript and approving it for publication was Zijian Zhang.

abandoned luggage detection and event classification. Experimental results indicate that the performance of BIVnet is superior to convolutional neural network architectures with a competitive complexity and reduced memory requirements. The rest of this manuscript is organized as follows: Section II describes the visual processing system in the brain as well as computational models of the human visual cortex. Section III presents the proposed network's structure and the learning algorithm. Section IV summarizes our experimental results and Section V concludes this paper.

II. BACKGROUND INFORMATION

Because our model has its roots in the biological visual processing system, we begin by describing the various structures in the brain involved in processing visual tasks, starting with the eye, retina and lateral geniculate nucleus up to the primary visual cortex [12].

A. THE VISUAL SYSTEM IN THE BRAIN

Anatomically, the eye is a three-layered structure comprising a lens. The innermost layer is the first neural-based module inside which the retina is suspended [13]. (The outer layer is an extension of the dura matter and the middle layer serves as a medium for blood nerves.) The retina is an association of neurons arranged in five alternating layers of synapses and interneurons. At a functional level, the retinal process extracts elementary features, such as boundaries, lines and basic shapes, from the visual input. Rather than levels of intensities, retinal neurons respond to patterns of lights rendering the structure an inherent feature extraction stage [14]. The optic nerves conduct information to the lateral geniculate nuclei (LGN) crossing at the optic chiasm. Each LGN is composed of a six-layered structure receiving projections from the retina in a retinotopic matter. As a result, any location in the visual field is mapped to a column of neurons projecting throughout the six layers of the nucleus. The nucleus is not fully connected: layers 1, 4 and 6 receive projections from the contralateral eye (the opposite hemisphere), while layers 2, 3, and 5 connect from the ipsilateral eye (the same hemisphere). The primary visual cortex receives connections from the LGN and projects processed visual information to higher order cortical areas. The extracted information includes orientation, color depth and motion. The primary visual cortex is characterized by a columnar organization in which cortical columns constitute the elementary computing unit. Increasingly complex information is extracted from input data to achieve robust invariant representations of visual information [15]. Figure 1 shows an illustration of the visual system in the brain starting from the eye to the primary visual cortex.

B. COMPUTATIONAL MODELS OF THE VISUAL CORTEX

Research focused on developing computational models of the visual cortex - as well as artificial structures inspired by the neural substrate - has spanned a wide range of applications such as action recognition [16], facial processing [17], motion perception [18], and early visual processing [19].

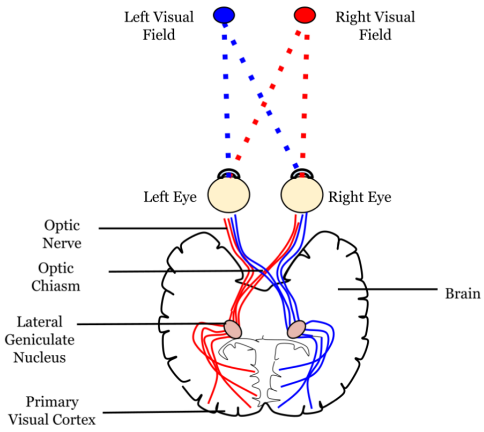

FIGURE 1. The visual system in the brain.

Some literature describing models that mimic the behavior of the visual cortex from its elementary structure to its large scale functionality exists. However, the neocognitron, convolutional neural network (CNN) and cortical algorithm (CA) models are the most prominent and closely related to our proposed model.

Proposed by Fukushima, the neocognitron [20] is one of the earliest computational models of the visual processing system. It consists of alternating layers of analog "S cells" and "C cells" in decreasing density. Inputs to these cells are firing at rates similar to those of biological neurons. S cells are of the inhibitory type while C cells receive projections for groups of S cells and are active when at least one of the input S cells is active. S-cells to C-cells connections are static while afferent connections to S cells are modular and iteratively learned throughout the training process. Early stages of the network act as a feature-extracting stage and learn in an unsupervised manner while higher stages perform complex tasks resulting from a supervised learning scheme. The network is characterized by an invariance to shift, rotation and scale. Unsupervised learning is achieved by strengthening a variable connection if the postsynaptic cell has the highest response in a predefined neighborhood and the presynaptic cell is active. Repeated exposure to patterns enables the network to extract discriminative aspects of categories without the need for feedback.

CNN are a very popular and powerful class of deep neural networks composed of a stack of convolutional and pooling layers [21]. The former performs a set of filtering processes to extract features from input images while the latter acts as a subsampling stage aimed at mapping regions of the visual field to subgroups of neurons. A classification stage, which is often a shallow architecture such as a multilayer perceptron (MLP), follows these stages of feature extraction. Characterized by a relatively low memory footprint, CNN have witnessed tremendous success in image classification [1], localization and detection [22], speech recognition [23] and a wide range of visual processing tasks [24].

CA are computational models inspired by the cortical organization of the primary visual cortex. These networks

comprise a six-layered structure where the elementary computational unit is the mini-column, an association of neurons sharing sensory input [25]–[27]. Connections in this network are of the horizontal and vertical types. The former connects columns within the same layer, providing an inhibitory link between neighboring columns rather than an information propagation medium while the latter connects consecutive layers. Training these networks occurs in two stages: an unsupervised stage which trains columns to respond to particular features of the input data, and a supervised phase to correct misrepresentations and create robust abstractions of the input data. A full mathematical description of CA can be found in [28], [29].

III. BIVNET MODEL

A. STRUCTURE

BIVnet is organized similarly to the visual processing system of the human brain. It starts with a 5-layer retinotopic structure mimicking the retina, projecting into a 6-layered network with similar structure to that of the LGN, and is followed by a 6-layered columnar-organized network with similar properties to the primary visual cortex. Our model exhibits several major differences from artificial neural networks. First, while traditional artificial neural networks employ the classical summation-activation-function model that generates a numerical output representing the combined input to the neuron, our model employs a more biologically plausible model characterized by an all or none response in which the magnitude is fixed while the pattern of firing encodes different input strengths. Unlike existing neural network models where excitation and inhibition alter the weight of a connection based on the response of the cell to an input, we adopt a more biologically plausible approach by hard-coding these processes in synapses mimicking the roles of gamma-Aminobutyric acid (GABA) and N-methyl-D-aspartate (NMDA) receptors defining the type of synapses in the neural substrate. While deep neural networks employ variants of gradient-descent (or error propagation) algorithms to learn the network's weights, we adopt a temporal-based Hebbian learning rule, which is primarily a spike-timing dependent plasticity (STDP) weight update rule that asymmetrically updates the weight of a synaptic connection according to the timing of the spike in the pre- or post-synaptic cell.

In addition, our model possesses some properties in common with those described in section II: (1) a retinotopic pattern as observed in CNNs, (2) excitatory and inhibitory synapses aligned with S and C cells of the neocognitron, and (3) a columnar organization as proposed in CA. Figure 2 is an illustration of the CNN, the neocognitron and BIVNet structures. Furthermore, Figure 3 shows the connections of the BIVnet retinal network with the retinotropic organization where columns throughout the network are mapped to areas of the visual field. This structure is also maintained in the LGN networks.

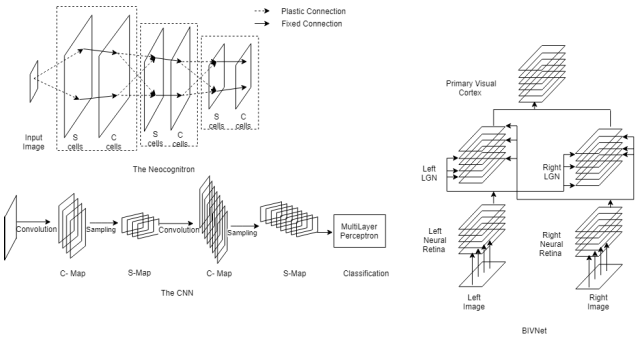

FIGURE 2. Comparison of CNN, Neocognitron and BIVNet structures.

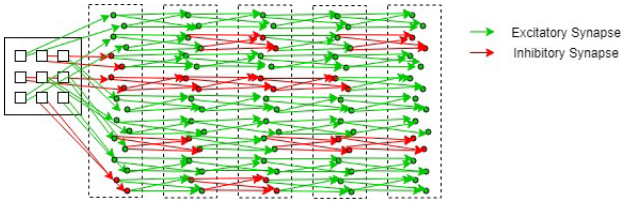

FIGURE 3. BIVnet retinal network with retinotropic mapping.

B. LEARNING ALGORITHM

Learning is the process through which neurons' synaptic weights are adjusted based on presented episodes; it allows the neural substrate to create and consolidate memory traces [30]. The neural basis of this phenomena can be attributed to the contributions of two procedures called potentiation and depression (also commonly denoted as strengthening and inhibiting, respectively), which result in opposing changes to the synaptic strength.

Mathematically, adaptation of synaptic strength has been successfully modeled via Hebbian models which explain both the activity-dependent learning and the competition mechanism that often drives small associations of neurons. These models facilitate connectivity between co-firing cells while decreasing that of non-simultaneously activated neurons [31]. In the time domain, Hebb's rule, which is also known as STDP, states that potentiation occurs when a pre-synaptic activity antecedes the firing of the post-synaptic cell in an excitatory synapse. Depression occurs when the opposite is true [32].

While accurate when describing the behavior of small populations of neurons, when characterizing larger associations' activity performing higher order functions such as working memory, human behavior involves a much more complex process in which reward and punishment play a crucial role. Growing evidence has shown that this reinforcement learning (RL) theory has been successfully employed to model dopamine-based reward learning in the brain [33], as well as interactions between neural associations such as the prefrontal cortex and the basal ganglia [34]–[36] plus the neural basis for a variety of neurological disorders [37], [38]. In this work, we propose a modification to the STDP framework which acts as a reinforcement learning strategy.

TABLE 1. Nomenclature.

Variable	Definition
X_i	set of parameter related to agent i
α	learning rate
a_i^t	action of agent i at time t
γ	decay parameter
ρ_i^t	probability of neuron i firing at time t
δ_i	refractory period of neuron i
y_i^t	output of neuron i at time t
η_{ij}^t	activity of j^{th} connection of neuron i at time t
f_i	probability density function of ρ_i^t
ϵ	firing threshold
$\Re$	reward signal
Ω_i	train of spikes generated by neuron i
τ_{ij}^t	rate of change in connection x_{ij}

We applied the online version of the Partially Observable Markov Decision Model (POMDP) reinforcement learning algorithm [39] to our model. A collection of interacting agents aimed at maximizing a common reward function is equivalent to each agent independently maximizing that function. Our nomenclature is summarized in Table 1. A set of parameters $X_i = [x_{i1}, \ldots, x_{ij}, \ldots]$ relevant to an agent i are updated according to the following:

$$x_{ij}^{t+\Delta t} = x_{ij}^t + \alpha \Re^{t+\Delta t} \tau_{ij}^{t+\Delta t} \tag{1}$$

$$\tau_{ij}^{t+\Delta t} = \gamma \tau_{ij}^t + \eta_{ij}^t \tag{2}$$

$$\eta_{ij}^t = \frac{1}{p_i^t(a_i)} \frac{\partial p_i^t(a_i)}{\partial x_{ij}^t} \tag{3}$$

where Δt is the time step, α is the learning rate parameter, τ is a trace depicting changes accumulated in η, and $p_i^t(a_i)$ denotes the probability of agent i choosing an action a_i at time t. In the case of our network, each neuron is modeled as an independent agent which, at each time step i, fires with a probability ρ. Hence takes an action $a_i = 1$ with a probability ρ_i^t or an action $a_i = 0$ with a probability $1 - \rho_i^t$. The neuron connects to a post-synaptic cell through a connection of synaptic strength x_{ij}, which is defined as positive for excitatory synapses and negative for inhibitory synapses. Hence,

$$\eta_{ij}^t = \begin{cases} \dfrac{1}{\rho_i^t} \dfrac{\partial \rho_i^t}{\partial x_{ij}} & if\ a_i^t = 1 \\ -\dfrac{1}{1-\rho_i^t} \dfrac{\partial \rho_i^t}{\partial x_{ij}} & if\ a_i^t = 0 \end{cases} \tag{4}$$

Equations (1), (2) and (4) define a reinforcement learning strategy based on a stochastic binary cell assumption. A neuron updates a connection weight as a linear function of the trace of the activity of this connection and the reward signal received. However, the elementary computing unit we adopted borrows the concept of strength encoding from the anatomy of the brain: stimulus strength is reflected at the neuronal output by the firing rate observed. In other words, a "strong input" leads to a higher frequency of spikes at the output of the neuron.

Mathematically, a neuron's output is described as

$$y_i^t = \delta_i^{t-t_i^h} + \sum_j x_{ij} \sum_{t_j^h \in \mathcal{T}} \theta_{ij}(t - t_i^h, t - t_j^h) \tag{5}$$

where t_i^h is the time of the last activity of the neuron belonging to the history of firing $\mathcal{T}$, δ_i represents the refractory period due to the last firing and t_j^h represents the history of the activity of the pre-synaptic cell antecedent to t. $x_{ij}\theta_{ij}(t-t_i^h, t-t_j^h)$ is the response of the post-synaptic neuron to the firing of the j^{th} pre-synaptic neuron at time t_j^h. In other words, a post-synaptic cell responds to the temporal summation of the firing of the collection of pre-synaptic neurons connected to it, taking into account a refractory period. From equation (5) we obtain

$$\frac{\partial y_i^t}{\partial x_{ij}} = \sum_{t_j^h \in \mathcal{T}} \theta_{ij}(t - t_i^h, t - t_j^h) \tag{6}$$

A variation of a neuron's output is therefore a function of change in activity of the neuron itself and that of the collection of pre-synaptic neurons connected to it.

Assuming a neuron fires with a probability $\rho_i^t = f_i(y_i^t - \epsilon$ where ϵ is the firing threshold and f_i is a probability density function, equation (4) can be written as

$$\eta_{ij}^t = \begin{cases} \dfrac{1}{f_i^t} \dot{f}_i^t \sum_{t_j^h \in \mathcal{T}} \theta_{ij}(t - t_i^h, t - t_j^h) & if\ a_i^t = 1 \\ -\dfrac{\Delta t}{1-f_i^t} \dot{f}_i^t \sum_{t_j^h \in \mathcal{T}} \theta_{ij}(t - t_i^h, t - t_j^h) & if\ a_i^t = 0 \end{cases} \tag{7}$$

Equation (7) describes the activity a connection x_{ij} undergoes as a function of the probability of a neuron firing and the temporal summation of the activity of pre-synaptic cells. In other words, the neurological basis of the reinforcement learning strategy presented here is encoded within the STDP as defined in equation (7).

Let us now consider the case where the firing rate of both pre- and post-synaptic cells are altered by a change in synaptic strength x_{ij}. The algorithm is applied to an agent formed by the post-synaptic cell i and all pre-synaptic cells j connected to it. Thus,

$$p_i(a_i)p_j(a_j) = \begin{cases} (1-\rho_i)(1-\rho_j) & if\ a_i = a_j = 0 \\ \rho_i(1-\rho_j) & if\ a_i = 1, a_j = 0 \\ (1-\rho_i)\rho_j & if\ a_i = 0, a_j = 1 \end{cases} \tag{8}$$

We defined the change in synaptic weight observed by a connection as a reinforcement learning problem governed by the firing rates of pre- and post-synaptic cells, which act as reinforcement learning agents whose action is described by neuronal activity.

The probability of both pre- and post-synaptic neurons firing simultaneously in a short interval Δt is negligible; therefore, we did not consider the case of $a_i = a_j = 1$. By analogy, we obtain

$$\eta_{ij}^t = \left(\frac{\Omega_i^t}{f_i^t} - 1\right) \frac{\partial f_i^t}{\partial x_{ij}} + \left(\frac{\Omega_j^t}{f_j^t} - 1\right) \frac{\partial f_j^t}{\partial x_{ij}} \tag{9}$$

TABLE 2. Datasets summary.

Dataset	# Classes	# Instances	Task
iLIDS-VID [40]	300	43800	Person Identification
Film Face	77	539	Person Identification
PETA [41]	8705	19000	Person Identification
Caviar [42]	2	65000	Abandoned luggage detection
UCF-Crime [43]	13	1900	Crime Classification

Therefore, a connection weight is changed following the occurrence of an activity η_{ij}, which is defined as a function of the series of spikes generated by both pre- and post-synaptic neurons. In other words, a connection conveying information from node i to node j is subject to change in the case of either neuron i or neuron j generating spikes. The case of both neurons firing simultaneously was not considered as the probability of such an event occurring is very low. If α and γ are chosen as larger than the decay time β of τ, taking the limit of Δt to zero, we obtain the following of equations to define the update rule under the STDP-based reinforcement learning strategy:

$$\frac{dx_{ij}}{dt} = \alpha \mathcal{R}^t \tau_{ij}^t \tag{10}$$

$$\beta \frac{d\tau_{ij}}{dt} = -\tau_{ij}^t + \eta_{ij}^t \tag{11}$$

$$\eta_{ij}^t = \left(\frac{\Omega_i^t}{f_i^t} - 1\right) \frac{\partial f_i^t}{\partial x_{ij}} + \left(\frac{\Omega_j^t}{f_j^t} - 1\right) \frac{\partial f_j^t}{\partial x_{ij}} \tag{12}$$

where Ω_i is the i^{th} neuron activity (i.e., the series of spikes produced by that neuron).

Equations (10), (11) and (12) define an STDP stochastic reinforcement learning strategy that alters the network's connections based on neuronal activity in a manner that mimics the biological properties of neurons.

IV. EXPERIMENTAL SECTION

In this section, we test our network's ability to perform three security-related tasks: person identification, abandoned luggage detection and classification of criminal behavior using the datasets summarized in Table 2. The video frames were extracted and preprocessed into images to use for the classification tasks. The proposed network was compared against Fukushima's neogcognitron and four CNN architectures pretrained on Imagenet: VGG16, resnet, mobilenet, and inception.

Table 3 summarizes the performance of the tested architectures in training and testing stages measured as accuracy and time, as well as relative improvement compared to BIVnet in percent (denoted Imp.). A positive number indicates superior performance compared to BIVnet while a negative number indicates degradation in performance compared to BIVnet. Figure 4 shows the average number of non-zero weights required to store the trained network (using a sparse representation) averaged across datasets. All results are based on a 4fold cross-validation scheme.

TABLE 3. Experimental results summary.

Dataset	Network	Train Acc.	Valid. Acc.	Test Acc.	Train. Time (min)	Imp.
i-LIDS	VGG16	0.998	0.99	0.98	3,720	0.5
	resnet	0.919	0.828	0.76	1,109	-21.5
	mobilenet	0.52	0.496	0.735	54	-24
	inception	0.834	0.918	0.965	165	-1
	Neocogn.	0.793	0.89	0.712	611	-26.3
	BIVNet	0.96	0.95	0.975	4,225	0
Film	VGG16	0.37	0.409	0.385	174	-37.7
	resnet	0.68	0.79	0.75	55	-1.2
	mobilenet	0.657	0.545	0.651	3	-11.1
	inception	0.182	0.513	0.513	8	-24.9
	Neocog.	0.553	0.438	0.524	28	-23.8
	BIVNet	0.732	0.85	0.762	210	0
PETA	VGG16	0.695	0.697	0.69	744	-6
	resnet	0.569	0.61	0.654	222	-9.6
	mobilenet	0.429	0.565	0.517	11	-23.3
	inception	0.567	0.717	0.51	33	-24
	Neocog.	0.379	0.492	0.501	122	-24.9
	BIVNet	0.729	0.78	0.75	845	0
Caviar	VGG16	0.927	0.954	0.897	1564	-8.8
	resnet	0.882	0.92	0.925	1043	-6
	mobilenet	0.922	0.886	0.854	80	-13.1
	inception	0.974	0.91	0.961	485	-2.4
	Neocog.	0.849	0.851	0.825	582	-16
	BIVNet	0.964	0.99	0.985	612	0
UCF	VGG16	0.755	0.949	0.738	1778	-12.7
	resnet	0.737	0.764	0.81	1225	-5.5
	mobilenet	0.806	0.643	0.616	319	-24.9
	inception	0.938	0.692	0.811	645	-5.4
	Neocog.	0.758	0.637	0.619	733	-24.6
	BIVNet	0.794	0.774	0.865	843	0

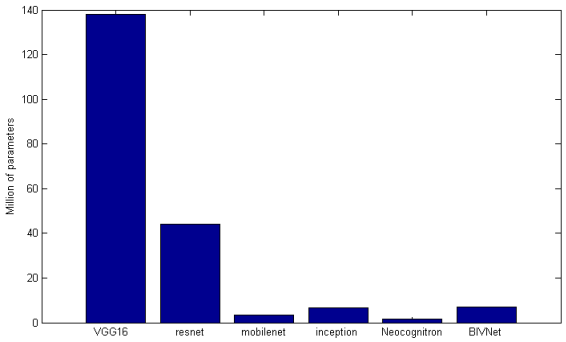

FIGURE 4. Complexity analysis overview of tested algorithms.

As shown in Table 3, our proposed algorithm outperformed five CNN architectures when used to examine the Film Face and PETA datasets and is competitive with the best state of the art architecture when used to assess the i-LIDS dataset for identification tasks. Regarding luggage detection tasks, BIVnet improved the state of the art accuracy achieved by inception by 2.4% with a slight increase in training time. Compared to VGG16, BIVnet improved accuracy by 8.8% for approximately 2.5× less training time. An improvement in accuracy ranging between 1.2% and 37.7% for the Film Face dataset is noted. The processing of other datasets increased in performance by an average of approximately 15.2% (averaged across datasets and architectures). Additionally, our network exhibited a considerable reduction

TABLE 4. Firing threshold sensitivity analysis.

Dataset	Firing Threshold	Test Accuracy	Training Time (min)	Number of parameters (M)
i-LIDS	0.1	0.535	4911	7.7
	0.4	0.975	4032	7.1
	0.7	0.575	2252	4.3
	1	0.414	1701	1.6
Film Face	0.1	0.207	286	4.2
	0.4	0.762	199	4.0
	0.7	0.404	111	2.3
	1	0.160	79	2.0
PETA	0.1	0.651	1122	5.8
	0.4	0.750	806	5.2
	0.7	0.517	280	4.5
	1	0.331	224	5.1
Caviar	0.1	0.414	581	8.4
	0.4	0.985	612	7.1
	0.7	0.581	274	6.2
	1	0.581	274	6.2
UCF-crime	0.1	0.422	1534	8.5
	0.4	0.981	822	7.1
	0.7	0.603	385	6.2
	1	0.328	200	0.4

in storage requirements as illustrated by the number of parameters with the exception of mobilenet, which is a network designed for low power mobile devices, and neocognitron, which exhibited considerably inferior performance compared to CNN and BIVnet. While the complexity of BIVnet may present a challenge in limited-resource environments (an average increase in training time of approximately $2\times$, $41\times$, $13\times$, and $3.5\times$ compared with resnet, mobilenet, inception and neocognitron, respectively), it must be noted that training occurs offline, thereby reducing the online burden to the prediction stage which involves propagating an input through the network. Given the much higher sparsity of our network (as illustrated by the reduced number of non-zero weights), storage and prediction both benefit from reduced complexity. Thus, given its reduced numbers of model parameters, BIVnet is sufficiently fast for predictions of novel instances. For example, BIVnet can be deployed in Internet of Things-type infrastructures where online computational resources are limited but real-time decision-making is a requirement.

Resnet's ability to achieve compelling performance when stacking multiple layers renders it competitive compared to BIVnet. The existing short connections in resnet reduces its training time compared to architectures of equal depth. However, the competitiveness of resnet compared to BIVnet cannot be generalized to all datasets as BIVnet achieves an improvement of 21.5% on i-LIDS. Although mobilenet's training time is considerably less than other architectures, especially BIVnet, its inferior performance is a major drawback. The variation in training time compared to BIVnet is due to a combination of database characteristics and architecture specifications, as well as the training algorithm parameters optimized per dataset. The considerable increase in training time for BIVnet compared to CNN architectures is a byproduct of several factors, including the number of instances, image resolution and task to be executed. The learning algorithm parameters also play a major role in training time; various optimal values are obtained for different datasets, thereby potentially affecting the training time differently.

Table 4 shows the effect of varying the firing threshold parameter on the performance of the proposed network by comparing the accuracy, training time, and number of parameters obtained for values of the firing threshold ranging from 0.1 to 1. As shown in Table 4, the optimal value of ϵ is approximately 0.4. The small firing threshold increases the number of parameters needed (more active connections) and thus, increases the training time required with a noticeable decrease in performance. A large firing threshold reduces the network's sparsity (neurons are less prone to firing, thus decreasing the competition between neurons) while degrading both the performance and training time.

V. CONCLUSION

This paper presents an image processing deep network called BIVnet that was inspired by the brain's visual system. A stochastic plasticity-dependent reinforcement learning algorithm is proposed to learn the weights between connections. The network was tested on three surveillance tasks, namely person identification, abandoned luggage detection and crime classification. Superior performance is demonstrated experimentally compared to state of the art models in addition to a marginal reduction in storage requirements at the expense of a moderate increase in training time, which can be performed offline.

REFERENCES

[1] A. Krizhevsky, I. Sutskever, and G. E. Hinton, "Imagenet classification with deep convolutional neural networks," in *Proc. Adv. Neural Inf. Process. Syst.*, 2012, pp. 1097–1105.
[2] Y. Wang, T. Bao, C. Ding, and M. Zhu, "Face recognition in real-world surveillance videos with deep learning method," in *Proc. 2nd Int. Conf. Image, Vis. Comput. (ICIVC)*, Jun. 2017, pp. 239–243.
[3] Y. Akbulut, A. Şengür, and S. Ekici, "Gender recognition from face images with deep learning," in *Proc. Int. Artif. Intell. Data Process. Symp. (IDAP)*, Sep. 2017, pp. 1–4.
[4] E. Ahmed, M. Jones, and T. K. Marks, "An improved deep learning architecture for person re-identification," in *Proc. IEEE Conf. Comput. Vis. Pattern Recognit.*, Jun. 2015, pp. 3908–3916.
[5] D. Li, X. Chen, Z. Zhang, and K. Huang, "Learning deep context-aware features over body and latent parts for person re-identification," in *Proc. IEEE Conf. Comput. Vis. Pattern Recognit.*, Jul. 2017, pp. 384–393.
[6] E. Ustinova, Y. Ganin, and V. Lempitsky, "Multi-region bilinear convolutional neural networks for person re-identification," in *Proc. 14th IEEE Int. Conf. Adv. Video Signal Based Surveill. (AVSS)*, Aug. 2017, pp. 1–6.
[7] S. Smeureanu and R. T. Ionescu, "Real-time deep learning method for abandoned luggage detection in video," 2018, *arXiv:1803.01160*. [Online]. Available: https://arxiv.org/abs/1803.01160
[8] A. Islam, Y. Zhang, D. Yin, O. Camps, and R. J. Radke, "Correlating belongings with passengers in a simulated airport security checkpoint," in *Proc. 12th Int. Conf. Distrib. Smart Cameras*, 2018, p. 14.
[9] S. Pouyanfar and S.-C. Chen, "Automatic video event detection for imbalance data using enhanced ensemble deep learning," *Int. J. Semantic Comput.*, vol. 11, no. 1, pp. 85–109, 2017.
[10] S. Bouindour, M. M. Hittawe, S. Mahfouz, and H. Snoussi, "Abnormal event detection using convolutional neural networks and 1-class SVM classifier," in *Proc. 8th Int. Conf. Imag. Crime Detection Prevention (ICDP)*, 2017, pp. 1–6.
[11] M. H. T. de Boer, H. Bouma, M. C. Kruithof, F. B. ter Haar, N. M. Fischer, L. K. Hagendoorn, B. Joosten, and S. Raaijmakers, "Automatic analysis of online image data for law enforcement agencies by concept detection and instance search," *Proc. SPIE*, vol. 10441, Oct. 2017, Art. no. 104410H.

[12] D. H. Hubel, "The visual cortex of the brain," *Sci. Amer.*, vol. 209, no. 5, pp. 54–63, 1963.
[13] N. J. Wade, "Image, eye, and retina (invited review)," *J. Opt. Soc. Amer. A, Opt. Image Sci.*, vol. 24, no. 5, pp. 1229–1249, 2007.
[14] R. H. Masland, "The neuronal organization of the retina," *Neuron*, vol. 76, no. 2, pp. 266–280, Oct. 2012.
[15] T. Vanderah and D. J. Gould, *Nolte's The Human Brain E-Book: An Introduction to Its Functional Anatomy*. Amsterdam, The Netherlands: Elsevier, 2015.
[16] N. Shu, Z. Gao, X. Chen, and H. Liu, "Computational model of primary visual cortex combining visual attention for action recognition," *PLoS ONE*, vol. 10, no. 7, 2015, Art. no. e0130569.
[17] B. A. Wandell, J. Winawer, and K. N. Kay, "Computational modeling of responses in human visual cortex," in *Brain Mapping: An Encyclopedic Reference*, vol. 1. Cambridge, MA, USA: Academic, 2015, pp. 651–659.
[18] P. Z. Eskikand, T. Kameneva, M. R. Ibbotson, A. N. Burkitt, and D. B. Grayden, "A biologically-based computational model of visual cortex that overcomes the X-junction illusion," *Neural Netw.*, vol. 102, pp. 10–20, Jun. 2018.
[19] D. A. Mély and T. Serre, "Towards a theory of computation in the visual cortex," in *Computational and Cognitive Neuroscience of Vision*. Singapore: Springer, 2017, pp. 59–84.
[20] K. Fukushima, S. Miyake, and T. Ito, "Neocognitron: A neural network model for a mechanism of visual pattern recognition," *IEEE Trans. Syst., Man, Cybern.*, vol. SMC-13, no. 5, pp. 826–834, Oct. 1983.
[21] Y. LeCun and Y. Bengio, "Convolutional networks for images, speech, and time series," in *The Handbook of Brain Theory and Neural Networks*, vol. 3361, no. 10. Cambridge, MA, USA: MIT Press, 1995, p. 1995.
[22] P. Sermanet, D. Eigen, X. Zhang, M. Mathieu, R. Fergus, and Y. LeCun, "OverFeat: Integrated recognition, localization and detection using convolutional networks," 2013, *arXiv:1312.6229*. [Online]. Available: https://arxiv.org/abs/1312.6229
[23] T. Sercu, C. Puhrsch, B. Kingsbury, and Y. LeCun, "Very deep multilingual convolutional neural networks for LVCSR," in *Proc. IEEE Int. Conf. Acoust., Speech Signal Process. (ICASSP)*, Mar. 2016, pp. 4955–4959.
[24] M. Nakada, H. Wang, and D. Terzopoulos, "AcFR: Active face recognition using convolutional neural networks," in *Proc. IEEE Conf. Comput. Vis. Pattern Recognit. Workshops (CVPRW)*, Jul. 2017, pp. 35–40.
[25] A. G. Hashmi and M. H. Lipasti, "Cortical columns: Building blocks for intelligent systems," in *Proc. IEEE Symp. Comput. Intell. Multimedia Signal Vis. Process. (CIMSVP)*, Mar. 2009, pp. 21–28.
[26] A. Hashmi, H. Berry, O. Temam, and M. Lipasti, "Automatic abstraction and fault tolerance in cortical microachitectures," *ACM SIGARCH Comput. Archit. News*, vol. 39, no. 3, pp. 1–10, Jun. 2011.
[27] A. Hashmi and M. H. Lipasti, "Discovering cortical algorithms," in *Proc. IJCCI*, 2010, pp. 196–204.
[28] N. Hajj and M. Awad, "A piecewise weight update rule for a supervised training of cortical algorithms," *Neural Comput. Appl.*, vol. 31, no. 6, pp. 1915–1930, 2017.
[29] N. Hajj and M. Awad, "Weighted entropy cortical algorithms for isolated Arabic speech recognition," in *Proc. Int. Joint Conf. Neural Netw. (IJCNN)*, Aug. 2013, pp. 1–7.
[30] W. Gerstner and W. M. Kistler, "Mathematical formulations of Hebbian learning," *Biological*, vol. 87, nos. 5–6, pp. 404–415, Dec. 2003.
[31] D. O. Hebb, *The Organization of Behavior: A Neuropsychological Theory*. Mahwah, NJ, USA: Lawrence Erlbaum, 1963.
[32] N. Caporale and Y. Dan, "Spike timing–dependent plasticity: A Hebbian learning rule," *Annu. Rev. Neurosci.*, vol. 31, pp. 25–46, Jul. 2008.
[33] K. M. Diederen, H. Ziauddeen, M. D. Vestergaard, T. Spencer, W. Schultz, and P. C. Fletcher, "Dopamine modulates adaptive prediction error coding in the human midbrain and striatum," *J. Neurosci.*, vol. 37, no. 7, pp. 1708–1720, 2017.
[34] J. P. O'Doherty, "Reward representations and reward-related learning in the human brain: Insights from neuroimaging," *Current Opinion Neurobiol.*, vol. 14, no. 6, pp. 769–776, 2004.
[35] P. Dayan and N. D. Daw, "Decision theory, reinforcement learning, and the brain," *Cogn., Affect., Behav. Neurosci.*, vol. 8, no. 4, pp. 429–453, 2008.
[36] M. Ito and K. Doya, "Multiple representations and algorithms for reinforcement learning in the cortico-basal ganglia circuit," *Current Opinion Neurobiol.*, vol. 21, no. 3, pp. 368–373, 2011.
[37] Q. J. M. Huys, T. V. Maia, and M. J. Frank, "Computational psychiatry as a bridge from neuroscience to clinical applications," *Nature Neurosci.*, vol. 19, no. 3, p. 404, 2016.
[38] S. Palminteri and M. Pessiglione, "Opponent brain systems for reward and punishment learning: Causal evidence from drug and lesion studies in humans," in *Decision Neuroscience*. Amsterdam, The Netherlands: Elsevier, 2017, pp. 291–303.
[39] J. Baxter and P. L. Bartlett, "Direct gradient-based reinforcement learning," in *Proc. IEEE Int. Symp. Circuits Syst. (ISCAS)*, Geneva, Switzerland, vol. 3, May 2000, pp. 271–274.
[40] M. Li, X. Zhu, and S. Gong, "Unsupervised person re-identification by deep learning tracklet association," 2018, *arXiv:1809.02874*. [Online]. Available: https://arxiv.org/abs/1809.02874
[41] Y. Deng, P. Luo, C. C. Loy, and X. Tang, "Pedestrian attribute recognition at far distance," in *Proc. 22nd ACM Int. Conf. Multimedia*, 2014, pp. 789–792.
[42] R. Fisher, J. Santos-Victor, and J. Crowley, *Context Aware Vision Using Image-Based Active Recognition*, document IST2001-3754, EC's Information Society Technology's Programme Project, 2001.
[43] W. Sultani, C. Chen, and M. Shah, "Real-world anomaly detection in surveillance videos," in *Proc. IEEE Conf. Comput. Vis. Pattern Recognit.*, 2018, pp. 6479–6488.

NADINE HAJJ was born in Beirut, Lebanon, in 1988. She received the B.E. degree in electrical and computer engineering from the Lebanese University, in 2010, and the M.E. and Ph.D. degrees in electrical and computer engineering from the American University of Beirut, in 2013 and 2019, respectively.

From 2010 to 2019, she was a Research Assistant with the Department of Electrical and Computer Engineering, American University of Beirut. From 2011 to 2012, she was a Graduate Research Intern with Intel Corporation, Hillsboro, OR, USA. She is the author of several articles in the fields of machine learning and artificial intelligence. Her research interests include multi-modal learning, deep learning, computational biology, and stochastic modeling.

MARIETTE AWAD received the Ph.D. degree in electrical engineering, in 2007. She is currently an Associate Professor with the Electrical and Computer Engineering Department, American University of Beirut. She has been a Visiting Professor with Virginia Commonwealth University, Intel Mobile Group, and MIT. She was invited by CVC labs, Google, and Qualcomm to present her work on machine learning and image processing. She has published a book *Efficient Machine Learning*, in 2015, as well as in numerous conferences and journals and is managing few grants. She is an Active Member in the IEEE and reviewer for the IEEE transactions. Prior to her academic position, she was with the IBM System and Technology Group, Vermont, as a Wireless Product Engineer, where she earned management recognition, several business awards, and multiple patents. Her current research interests include machine learning, data analytics, and the Internet of Things.